Available online at www.synsint.com

Synthesis and Sintering

ISSN 2564-0186 (Print), **ISSN** 2564-0194 (Online)

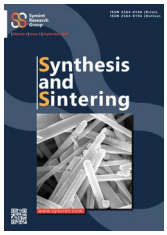

Research article

Enhanced methyl green adsorption of ZIF-8 metal-organic framework: Insights from different solvents

Saeid Zahedi Asl [a], **Fahimeh Hooriabad Saboor** [a,b,*]

[a] *Department of Chemical Engineering, Faculty of Engineering, University of Mohaghegh Ardabili, Ardabil 5619911367, Iran*
[b] *Energy Management Research Center, University of Mohaghegh Ardabili, Ardabil, Iran*

A B S T R A C T

This study investigates the effect of solvent type on the structural properties and adsorption performance of the ZIF-8 metal-organic framework for removing various dyes including, methyl green (MG), methylene blue (MB), and methyl orange (MO) from water in acidic and alkaline environments. ZIF-8 samples were synthesized using zinc nitrate, methylimidazole, and three different solvents including, water, methanol, and ethanol under atmospheric pressure and 70 °C. Characterization using BET, XRD, FT-IR, and TGA techniques sheds light on the structural, chemical, and thermal properties of ZIF-8 samples. Among the samples, ZIF-8/M, synthesized using methanol, stands out, demonstrating the high surface area of 2172.7 m^2/g, large total pore volume of 1.5412 cm^3/g, and high crystallinity of 31.9% with improved thermal stability. Furthermore, ZIF-8/M shows better adsorption performance for methyl green with a removal percentage of 81.9%, 87.1%, and an adsorption capacity of 20.5 mg/g and 21.8 mg/g, in acidic and alkaline environments, respectively. Enhanced dye adsorption of ZIF-8/M is associated with both physical and effective chemical adsorption mechanisms via tuning the environment's acidity.

KEYWORDS

ZIF-8
Metal-organic framework
Solvent effect
Dye adsorption
Methyl green

OPEN ACCESS

1. Introduction

Water is a vital resource, covering 71% of the earth's surface, while the remaining 29% is land. Of the 71% water available, 97% is saline, and only 3% is freshwater [1]. However, a significant portion of this freshwater is trapped in glaciers and frozen regions, making it inaccessible [2]. In addition to the scarcity of fresh water, a significant portion of it became practically unusable due to various pollutants. Synthetic dyes, organic and non-biodegradable pollutants, are among the most significant water contaminants due to their extensive use in various industries [3]. Also, dyes are classified based on chemical structure, source, solubility, and application [4]. The presence of dyes in the aquatic environment poses serious health risks to humans, as many synthetic dyes are toxic, potentially carcinogenic, and can cause allergic reactions [5]. From an environmental perspective, dyes in water can block sunlight, disrupting aquatic ecosystems and hindering photosynthesis in aquatic plants. This, in turn, reduces oxygen levels and adversely affects fish and other aquatic organisms [6].

Removing dyes from water is crucial to prevent long-term environmental damage and protect human health [7]. The adsorption method is considered the optimal technique for water treatment due to its high efficiency, ease of operation, economic feasibility, and environmental compatibility. In contrast, the other treatment techniques, such as photocatalytic degradation, sonochemical degradation, membranes, and biological treatment, mostly suffer from complex systems and high operational costs [8, 9].

Metal-organic frameworks, made of metal ions or clusters and organic ligands, are considered novel and effective crystalline materials with one-, two-, or three-dimensional structures for use in water treatment [10]. Their large surface area, high porosity, adjustable

* Corresponding author. *E-mail address:* f.saboor@uma.ac.ir (F. Hooriabad Saboor)
Received 24 August 2024; Received in revised form 26 September 2024; Accepted 27 September 2024.

https://doi.org/10.53063/synsint.2024.43244

structure/functionality, non-toxicity, water stability, and tunable hydrophilicity/hydrophobicity make them a promising candidate in the adsorption and separation processes [11]. Specifically, ZIF-8 is regarded as one of the most effective MOFs for dye adsorption, thanks to its large surface area, non-toxic nature, excellent thermal and structural stability, and reusability [12].

The role of solvents in ZIF-8 synthesis is crucial due to their significant impact on the crystalline structure and pore morphology of metal-organic frameworks. Specifically, solvents play a crucial role in the nucleation and crystal growth rate, the size and shape of the crystals, and the surface properties and porosity of the final material [13]. Using protic solvents such as water, methanol, and ethanol in the synthesis can lead to MOFs with different physical and chemical properties. The strength of the hydrogen bonds between solvent molecules and ligands in MOF structure plays a vital role in their formation and properties. Zhang et al. [14] studied the effect of water/ethanol solvent in the synthesis of $Cu_3(BTC)_2$. They demonstrated that using ethanol in low amounts or its absence impedes the formation of the crystalline structure in metal–organic frameworks. However, increasing the ethanol content to more than 30%, results in the successful synthesis of $Cu_3(BTC)_2$ at room temperature. Moreover, the crystal size of MOFs can be adjusted by modifying the solvent type and content.

Existing literature emphasizes that solvent variations significantly impact the synthesis and properties of metal–organic frameworks (MOFs). In our study, we aimed to elucidate the influence of three different solvents including water, ethanol, and methanol on the structural, chemical, and thermal properties of ZIF-8. Additionally, we investigated its adsorption performance for methyl green (MG) removal from water, comparing it with methylene blue (MB) and methyl orange (MO) dyes. Comprehensive analyses using XRD (X-ray diffraction), BET (Brunauer-Emmett-Teller), FTIR (Fourier-transform infrared spectroscopy), and TGA (Thermogravimetric analysis) characterized the properties of the ZIF-8 samples.

2. Materials and methods

2.1. Materials

The chemicals including zinc nitrate hexahydrate ($Zn(NO_3)_2.6H_2O$; Merck, 99%), 2-methylimidazole ($H_3C_3H_2N_2H$; Merck, 99%), ethanol (C_2H_5OH; Merck, 99.9%), methanol (CH_3OH; Merck, 99.9%), methyl orange ($C_{14}H_{14}N_3NaO_3S$; Merck, Reag. Ph Eur standard), methyl green ($C_{26}H_{33}Cl_2N_3$; British drug houses, for microscopy), methylene blue ($C_{16}H_{18}ClN_3S$; Merck, Reag. Ph Eur standard), and deionized water (DI) were used in this study as received without any further purification.

2.2. Synthesis of ZIF-8

Fig. 1 shows the schematic of the ZIF-8 synthesis method. In a typical synthesis, a specific amount of zinc nitrate hexahydrate and 2-methylimidazole, as the metal precursor and organic ligand, respectively, were mixed in 60 ml of each solvent, including water, methanol, and ethanol.

This mixture was placed in a water bath of 70 °C for a specified duration to complete the synthesis of the metal-organic framework. The mole ratio of metal to ligand is set to 1:10 in all samples. The resulting milky solution was separated using a centrifuge at 10000 rpm for 5 min, followed by washing several times with DI water. The final wet solid was dried in an oven at 60 °C overnight. The samples were designated as ZIF-8/M, ZIF-8/E, and ZIF-8/W, corresponding to the ones synthesized in the methanol, ethanol, and water, respectively.

In the synthesis process of ZIF-8, zinc nitrate ($Zn(NO_3)_2$) serves as the source of Zn^{2+} ions, while 2-methylimidazole functions as the organic ligand. Initially, zinc nitrate dissolves in solution, dissociating into Zn^{2+} and NO_3^- ions. Simultaneously, 2-methylimidazole undergoes deprotonation, transforming into imidazolate anions acting as ligands. These imidazolate ions coordinate with Zn^{2+} forming a tetrahedral structure that constitutes the core of the zeolitic framework. Solvents such as methanol, ethanol, or water play a crucial role in dissolving the reactants and controlling the crystallization process. The reaction forms a porous, crystalline ZIF-8 structure, where Zn^{2+} ions are bridged by multiple imidazolate ligands, creating a stable framework [15, 16].

2.3. Characterization

The characteristics of the synthesized ZIF-8 samples were analyzed using N_2 adsorption-desorption at 77 K (Brunauer-Emmett-Teller (BET); BELSORP mini II), X-ray diffraction (XRD; Rigaku Ultima

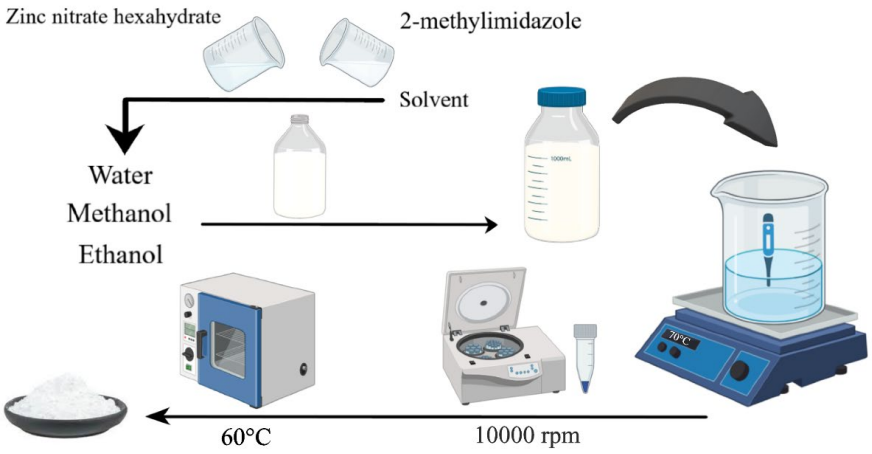

Fig. 1. Schematic of ZIF-8 synthesis method.

IV), Fourier Transform Infrared Spectroscopy (FT-IR; PerkinElmer/LX185256), and Thermogravimetric Analysis (TGA; Linseis/STA PT-1000) techniques.

BET analysis assessed the specific surface area, pore volume, and average pore diameter of the three samples. Sample degassing was carried out at 100 °C for 9 hours. The crystallinity of ZIF-8 samples was calculated based on XRD data using the following equation [17]:

$$\text{Crystallinity } (\%) = \frac{\text{The area under the characteristic peaks}}{\text{Total area under the chart}} \times 100 \quad (1)$$

FTIR was carried out in the 400 to 4000 cm^{-1} range to analyze the chemical bonds and functional groups in MOF structure. TGA was used to evaluate the thermal stability of ZIF-8 samples in the temperature range of 0 to 700 °C.

Furthermore, a UV-Vis spectrophotometer (Nanolytik /NanoSpec 2 UV-A) was used to measure the dye absorbance and calculate the dye concentration in solutions.

2.4. Dye adsorption experiments

Methyl orange, methylene blue, and methyl green dyes were used to test the adsorption performance of the ZIF-8 sample. Experiments were conducted in acidic (pH=5) and alkaline (pH=9) environments. Dye solutions with a concentration of 25 ppm were prepared and poured into closed containers with a volume of 10 ml. Next, 10 mg of ZIF-8 adsorbent was added to each container, and the containers were placed on a shaker set at 250 rpm for 30 minutes.

Afterward, the adsorbent was separated, and the concentration of the remaining dye was measured using the UV-Vis spectrophotometer. The concentration of the dyes in the solution was calculated using the calibration curves presented in Fig. S1. Each dye's color removal percentage and adsorption capacity were computed using Eqs. 2 & 3, respectively.

$$\text{Removal percent } (\%) = \frac{C_0 - C_e}{C_0} \times 100 \quad (2)$$

$$\text{Adsorption capacity } (mg/g) = \frac{(C_0 - C_e)v}{m} \times 100 \quad (3)$$

where C_0 represents the initial concentration of dye in the solution (in ppm), C_e is the dye concentration in the solution after an adsorption time (in ppm), v is the solution volume (in ml), and m is the adsorbent mass (in mg) used in each test. Using Eqs. 2 & 3, the effectiveness of the ZIF-8 sample in reducing dye concentration can be determined [18].

3. Results and discussion

3.1. Characterization results

Fig. 2a displays the XRD patterns of ZIF-8 compounds synthesized using various solvents. All the characteristic peaks of ZIF-8 at 7.21 °, 10.43 °, 12.78 °, 14.82 °, 16.48 °, and 18.15 ° are observed in the ZIF-8/E and ZIF-8/M samples [19]. However, the ZIF-8/M sample exhibits a narrower peak width compared to the ZIF-8/E sample, suggesting higher crystallinity. Specifically, the ZIF-8/M sample demonstrates approximately 31.9% crystallinity, as indicated in Table 1.

In contrast, the ZIF-8/W sample does not display these characteristic peaks, suggesting that the synthesis of ZIF-8 was not well executed, attributed to the impurities in the solution mixture. The crystallinity of the ZIF-8/W sample is calculated using only a limited number of characteristic peaks, resulting in significantly lower crystallinity than the other samples.

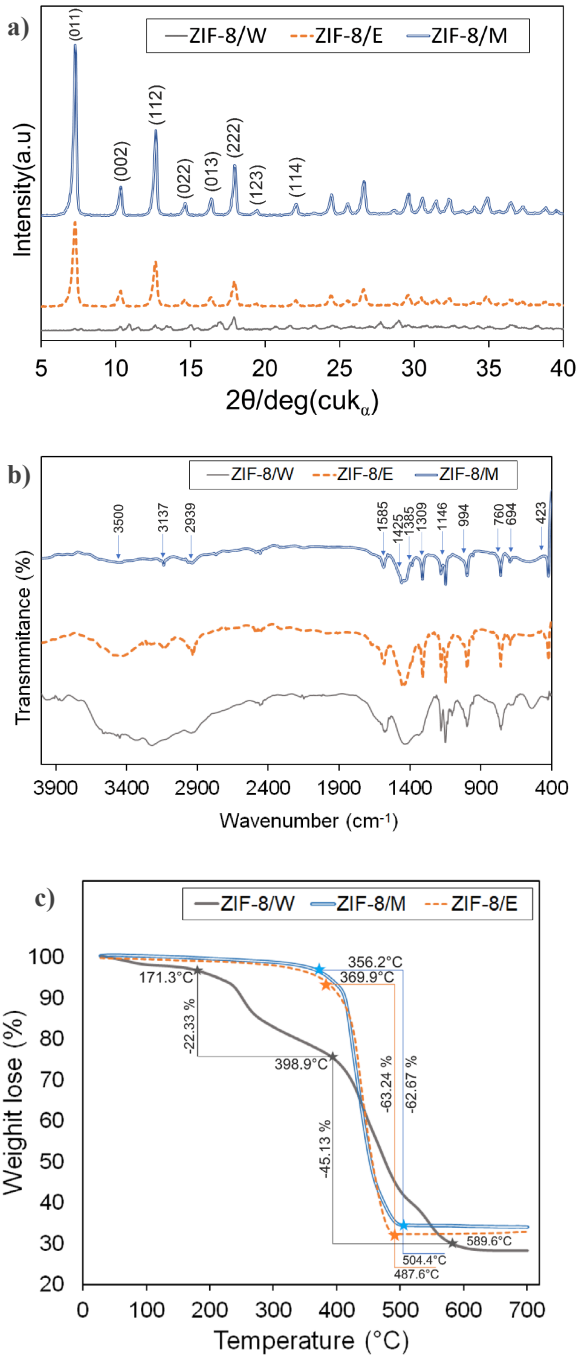

Fig. 2. Analysis results of a) XRD, b) FTIR, and c) TGA.

The FT-IR spectra of the ZIF-8 samples, presented in Fig. 2b, reveal several characteristic bands at 3455, 3137, 2939, 1585, 1458, 1425, 1385, 1309, 1146, 995, 760, 694, and 423 cm^{-1} of ZIF-8 structure. These observed bands align with previously reported data in the literature [20]. The stretching vibration band at 423 cm^{-1} indicates the Zn–N bond, confirming the chemical interaction between zinc ions and

Table 1. Structural properties of ZIF-8 samples using BET and XRD data.

Sample	Specific surface area (m^2/g)	Total pore volume (cm^3/g)	Crystallinity (%)
ZIF-8/W	268.1	0.137	10.8
ZIF-8/M	2172.7	1.541	31.9
ZIF-8/E	1327.8	1.336	28.8

nitrogen atoms within the methylimidazole groups. The 3455 cm^{-1} band corresponds to the O–H stretching from moisture in KBr. The peaks at 3137 cm^{-1} and 2939 cm^{-1} correspond to the asymmetric stretching vibrations of C–H bonds in aromatic and aliphatic structures, respectively. The 1585 cm^{-1} band represents the C=N stretching vibration. Bands within the 1300–1460 cm^{-1} range are attributed to whole-ring stretching vibrations, and the 1146 cm^{-1} band corresponds to aromatic C–N stretching. The bands observed at 995 cm^{-1} and 760 cm^{-1} are linked to the bending vibrations of C–N and C–H, respectively. Additionally, the band at 694 cm^{-1} corresponds to the out-of-plane bending of the ligand ring [21].

The results of the TG analysis for the three synthesized ZIF-8 samples are shown in Fig. 2c. The significant weight loss observed in all samples at approximately 400–450 °C can be attributed to the decomposition of the metal-organic framework. However, the onset of decomposition for the ZIF-8/W sample occurs at a lower temperature, and this sample exhibits more significant weight loss up to 450 °C. This could be due to the presence of impurities and a weaker structure. The ZIF-8/M and ZIF-8/E samples show higher thermal stability, with decomposition beginning at higher temperatures. These results indicate that using methanol and ethanol as solvents leads to the synthesis of ZIF-8 with higher thermal stability and more robust structural integrity.

Fig. 3a & b show N_2 adsorption-desorption isotherms and pore size distribution using BJH method of ZIF-8/M, ZIF-8/E and ZIF-8/W samples. As shown in Fig. 3a, all samples typically display type I N_2 adsorption-desorption isotherms. Moreover, a hysteresis loop of type H1 is observed in the isotherms of ZIF-8/M and ZIF-8/E samples. The H1-type hysteresis loop is usually associated with mesoporous systems with uniform and ordered cylindrical or near-cylindrical pores [22, 23]. This hysteresis type is mainly observed in N_2 adsorption-desorption isotherms where the mesopores have a uniform size distribution. It typically appears as a loop with a small distance between the adsorption and desorption curves, without sudden changes or sharp slopes relative to each other [24]. However, for the ZIF-8/W sample such a hysteresis loop is not observed. This may be because ZIF-8/W has very small pores, or its pore structure is such that the processes of filling and emptying the pores are almost similar.

The pore size distribution of the ZIF-8 samples was calculated using the BJH method and is represented in Fig. 3b. For ZIF-8/M and ZIF-8/E samples both micro- and meso-pores are observed with peaks at about 45 nm and 10 nm, respectively. In comparison, the majority of the pores are larger than 2 nm. For the ZIF-8/W sample, there is no microporosity observed, which is consistent with its low BET surface area and low crystallinity.

The specific surface area, pore volume and mean pore diameter data calculated using the BET method are presented in Table 1.

The ZIF-8/M sample has the highest specific surface area of about 2172 m^2/g and a total pore volume of 1.54 cm^3/g. These data indicate the formation of highly porous structures with high surface areas using methanol as a solvent. The small size of methanol molecules, low viscosity, and high solubility results in faster dispersion and diffusion in the synthesis mixture, leading to high nucleation density and porosity [25]. The ZIF-8/W sample has the lowest specific surface area due to hydrolysis in the presence of water, which reduces the synthesis efficiency and leads to the formation of less porous structures. Additionally, the larger average pore diameter in ZIF-8/E can be attributed to ethanol's influence on facilitating crystal growth rather than nucleation rate [26].

Moreover, in the ZIF-8 synthesis process, water can lead to hydrolysis of the reactants; especially zinc nitrate and 2-methylimidazole. Hydrolysis is a chemical reaction where water breaks down the chemical bonds of the reactants, leading to the formation of unwanted by-products or incomplete reactions. This can result in the formation of ZIF-8 with lower crystallinity, reduced surface area, and less well-defined porous structures, as the intended coordination between zinc ions and the organic linker is disrupted [27].

3.2. Dye adsorption performance

Based on the exceptional structural and chemical properties of the ZIF-8/M sample, as detailed in section 3.1, we examined its adsorption performance for removing MG, MB, and MO from water under both acidic (pH=5) and alkaline (pH=9) conditions.

Fig. 4 a–c displays UV-Vis absorption spectra of MB, MG, and MO

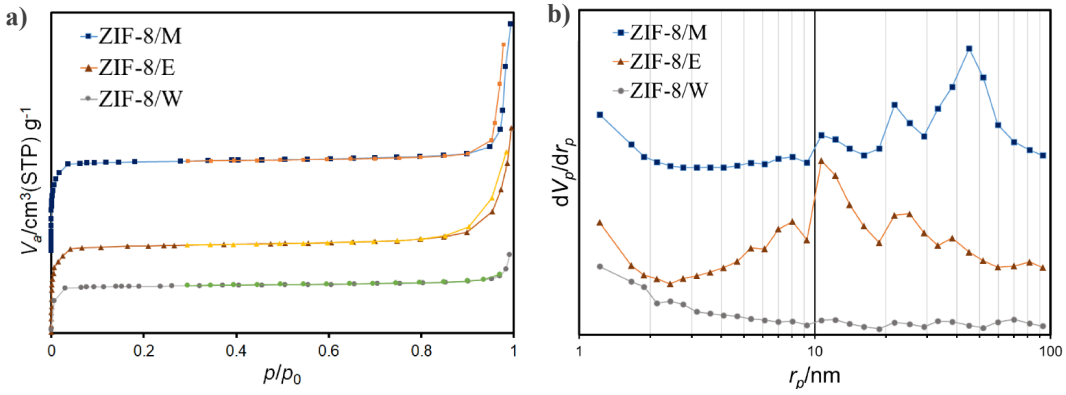

Fig. 3. a) N_2 adsorption-desorption isotherms and b) BJH pore size distribution for ZIF-8 samples.

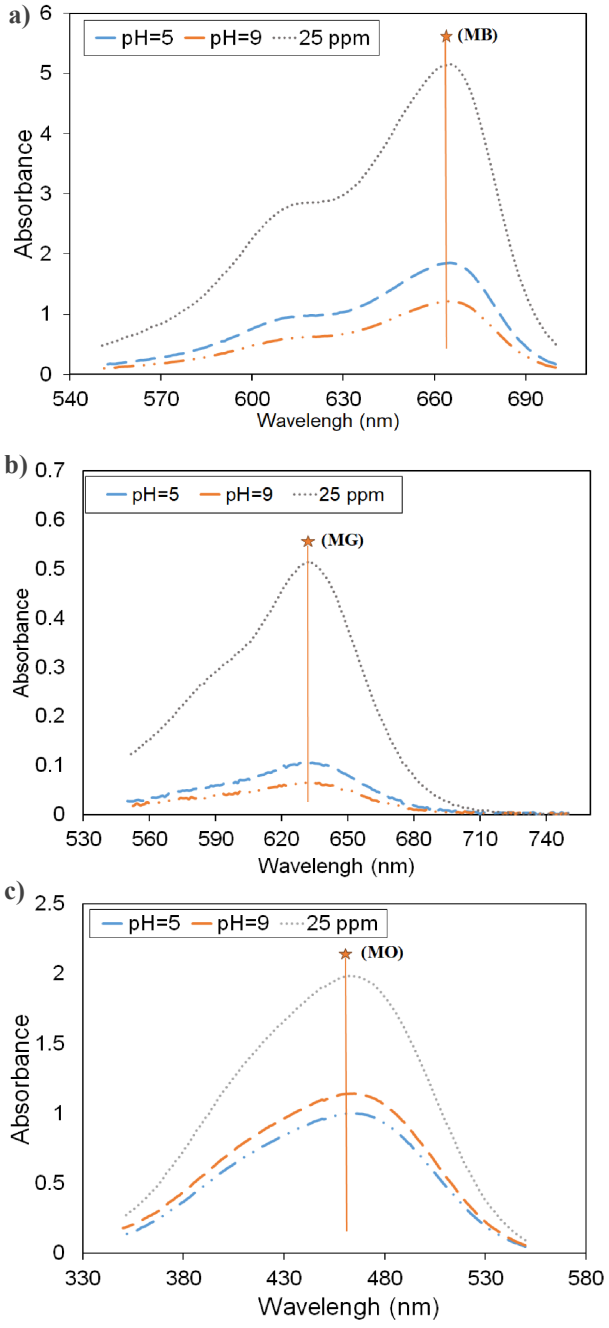

Fig. 4. UV-visible absorption spectra of a) MB, b) MG, and c) MO dyes before and after the adsorption test for the ZIF-8/M sample.

dye solutions (25 ppm) before and after the adsorption experiments. Maximum absorption peaks of MB, MG, and MO are at 646, 633, and 464 nm, respectively. As shown in Fig. 4 a–c, the UV-Vis absorption peak significantly reduces after the addition of ZIF-8 adsorbent, revealing a decrease in the concentration of dyes. Specifically, methylene blue and methyl green exhibit higher absorbance at pH=9 compared to pH=5, contrasting with the absorption behavior of MO. Moreover, the drop in the absorption peak for MG after adding the ZIF-8 sample is more significant compared with the other dyes.

The removal percent and adsorption capacity results, calculated using Eqs. 2 & 3 are presented in Table 2. The adsorption experimental

Table 2. The removal percentage of MB, MO, and MG dyes at 25 ppm in both acidic and basic environments using ZIF-8/M.

Solution condition	Dye	Removal percent (%)	Adsorption capacity (mg/g)
pH=5	MB	64.4	16
	MO	42.4	10.6
	MG	81.9	20.5
pH=9	MB	76.2	19.1
	MO	41.3	10.3
	MG	87.1	21.8

results show that in acidic conditions, the removal percentages of methylene blue and methyl green are 64.6% and 81.9%, respectively, while in basic conditions, these values increase to 76.2% and 87.1%. Conversely, the removal percentage of methyl orange slightly decreases from 42.43% in acidic solution to 41.3% in basic solution. Considering the point of zero charge (pH_{pzc}) of ZIF-8, which is 9, and the electrochemical properties of the dyes, in the acidic solution (pH=5), the ZIF-8 surface carries a positive charge, which reduces the effectiveness of cationic dye adsorption such as methylene blue and methyl green, because of electrostatic repulsion between the adsorbent and these dyes [28]. In contrast, the adsorption of methyl orange as an anionic dye is more efficient under acidic conditions. The negatively charged surface of ZIF-8 in alkaline solutions with pH≥9 enhances the adsorption of cationic dyes due to electrostatic attraction. These findings emphasize the influence of pH and the adsorbent's surface charge on dye removal efficiency and highlight the critical role of pH adjustment in optimizing the adsorption process.

According to literature [29], the maximum adsorption of MO usually occurs at acidic conditions with pH of 2 and the adsorption capacity does not change significantly with increasing pH value from 5 to 9 that reveals negligible changes in adsorbent surface charges [28]. Table 3 represents a comparative analysis of various MOFs used in dye adsorption, various dyes, and maximum adsorption capacities. The current study shows enhanced adsorption performance for MG compared with literature.

Table 3. Comparative analysis of various MOFs used in dye adsorption.

Adsorbent	Dye	Maximum adsorption capacity (mg/g)	Ref.
ZIF-8	MO	19.4	[30]
ZIF-8	MO	322.58	[31]
ZIF-8	MB	10.3	[32]
ZIF-8	MB	522.95	[33]
ZIF-8	MB	205	[34]
ZIF-8	MB	3	[35]
ZIF-67	MG	4.8	[36]
ZIF-8/M	MB	19.7	This work
ZIF-8/M	MO	10.6	This work
ZIF-8/M	MG	21.8	This work

4. Conclusions

The ZIF-8 metal-organic framework was synthesized using three different solvents including water, methanol, and ethanol, and characterized using BET, XRD, FT-IR, and TGA analyses. The findings demonstrate that the choice of solvent significantly influences the crystallinity, crystal structure, specific surface area, porosity, and thermal stability of ZIF-8. The results revealed that ZIF-8/M exhibited the highest crystallinity, BET surface area, and thermal stability. This is attributed to methanol's ability to promote the formation of smaller, more porous crystals. In contrast, ZIF-8/W displayed lower crystallinity and surface area, resulting in less efficient synthesis and the formation of less porous structures due to the hydrolysis. Furthermore, adsorption experiments using the synthetic dyes methylene blue, methyl orange, and methyl green highlighted the potential of ZIF-8 as an effective MG adsorbent. Under basic conditions (pH=9), ZIF-8 exhibited higher cationic dye adsorption dye due to electrostatic attractions, whereas under acidic conditions (pH=5), anionic dye adsorption was more effective. These results emphasize the critical role of adsorbent structure and solution pH in optimizing the adsorption process.

CRediT authorship contribution statement

Saeid Zahedi Asl: Conceptualization, Methodology, Writing – original draft & editing.
Fahimeh Hooriabad Saboor: Writing – review & editing, Supervision.

Data availability

The data underlying this article will be shared on reasonable request to the corresponding author.

Declaration of competing interest

The authors declare no competing interests.

Funding and acknowledgment

The authors received no financial support for the research, authorship, and/or publication of this article.

References

[1] R.K. Mishra, Fresh water availability and its global challenge, Br. J. Multidiscip. Adv. Stud. 4 (2023) 1–7. https://doi.org/10.37745/bjmas.2022.0207.
[2] A. Ahmad, T. Azam, Water purification technologies, Bottled and Packaged Water, Woodhead Publishing. (2019) 83–120. https://doi.org/10.1016/B978-0-12-815272-0.00004-0.
[3] L. Rani, J. Kaushal, A.L. Srivastav, P. Mahajan, A critical review on recent developments in MOF adsorbents for the elimination of toxic heavy metals from aqueous solutions, Environ. Sci. Pollut. Res. 27 (2020) 44771–44796. https://doi.org/10.1007/s11356-020-10738-8.
[4] J. Kaushal, P. Mahajan, N. Kaur, A review on application of phytoremediation technique for eradication of synthetic dyes by using ornamental plants, Environ. Sci. Pollut. Res. 28 (2021) 67970–67989. https://doi.org/10.1007/s11356-021-16672-7.
[5] H. Solayman, M.A. Hossen, A. Abd Aziz, N.Y. Yahya, K.H. Leong, et al., Performance evaluation of dye wastewater treatment technologies: A review, J. Environ. Chem. Eng. 11 (2023) 109610. https://doi.org/10.1016/j.jece.2023.109610.
[6] R. Al-Tohamy, S.S. Ali, F. Li, K.M. Okasha, Y.A.-G. Mahmoud, et al., A critical review on the treatment of dye-containing wastewater: Ecotoxicological and health concerns of textile dyes and possible remediation approaches for environmental safety, Ecotoxicol. Environ. Saf. 231 (2022) 113160. https://doi.org/10.1016/j.ecoenv.2021.113160.
[7] A.K. Alsukaibi, Various approaches for the detoxification of toxic dyes in wastewater, Processes. 10 (2022) 1968. https://doi.org/10.3390/pr10101968.
[8] V.K.-M. Au, Recent advances in the use of metal-organic frameworks for dye adsorption, Front. Chem. 8 (2020) 708. https://doi.org/10.3389/fchem.2020.00708.
[9] N. Singh, G. Nagpal, S. Agrawal, Water purification by using adsorbents: a review, Environ. Technol. Innov. 11 (2018) 187–240. https://doi.org/10.1016/j.eti.2018.05.006.
[10] V.F. Yusuf, N.I. Malek, S.K. Kailasa, Review on metal–organic framework classification, synthetic approaches, and influencing factors: applications in energy, drug delivery, and wastewater treatment, ACS Omega. 7 (2022) 44507–44531. https://doi.org/10.1021/acsomega.2c05310.
[11] D. Jiang, M. Chen, H. Wang, G. Zeng, D. Huang, et al., The application of different typological and structural MOFs-based materials for the dyes adsorption, Coord. Chem. Rev. 380 (2019) 471–483. https://doi.org/10.1016/j.ccr.2018.11.002.
[12] Z. Pouramini, S.M. Mousavi, A. Babapoor, S.A. Hashemi, C.W. Lai, et al., Effect of metal atom in zeolitic imidazolate frameworks (ZIF-8 & 67) for removal of dyes and antibiotics from wastewater: a review, Catalysts. 13 (2023) 155. https://doi.org/10.3390/catal13010155.
[13] R. Seetharaj, P. Vandana, P. Arya, S. Mathew, Dependence of solvents, pH, molar ratio and temperature in tuning metal organic framework architecture, Arab. J. Chem. 12 (2019) 295–315. https://doi.org/10.1016/j.arabjc.2016.01.003.
[14] B. Zhang, J. Zhang, C. Liu, X. Sang, L. Peng, et al., Solvent determines the formation and properties of metal–organic frameworks, RSC Adv. 5 (2015) 37691–37696. https://doi.org/10.1039/C5RA02440D.
[15] K.S. Park, Z. Ni, A.P. Côté, J.Y. Choi, R. Huang, et al., Exceptional chemical and thermal stability of zeolitic imidazolate frameworks, Proc. Natl. Acad. Sci. 103 (2006) 10186–10191. https://doi.org/10.1073/pnas.0602439103.
[16] R. Banerjee, H. Furukawa, D. Britt, C. Knobler, M. O'Keeffe, O.M. Yaghi, Control of pore size and functionality in isoreticular zeolitic imidazolate frameworks and their carbon dioxide selective capture properties, J. Am. Chem. Soc. 131 (2009) 3875–3877. https://doi.org/10.1021/ja809459e.
[17] M. S'ari, H. Blade, S. Cosgrove, R. Drummond-Brydson, N. Hondow, et al., Characterization of amorphous solid dispersions and identification of low levels of crystallinity by transmission electron microscopy, Mol. Pharm. 18 (2021) 1905–1919. https://doi.org/10.1021/acs.molpharmaceut.0c00918.
[18] Y. Miyah, A. Lahrichi, M. Idrissi, S. Boujraf, H. Taouda, F. Zerrouq, Assessment of adsorption kinetics for removal potential of Crystal Violet dye from aqueous solutions using Moroccan pyrophyllite, J. Assoc. Arab Univ. Basic Appl. Sci. 23 (2017) 20–28. https://doi.org/10.1016/j.jaubas.2016.06.001.
[19] A. Paul, G. Vyas, P. Paul, D.N. Srivastava, Gold-nanoparticle-encapsulated ZIF-8 for a mediator-free enzymatic glucose sensor by amperometry, ACS Appl. Nano Mater. 1 (2018) 3600–3607. https://doi.org/10.1021/acsanm.8b00748
[20] J. Cravillon, S. Münzer, S.-J. Lohmeier, A. Feldhoff, K. Huber, M. Wiebcke, Rapid room-temperature synthesis and characterization of nanocrystals of a prototypical zeolitic imidazolate framework, Chem. Mater. 21 (2009) 1410–1412. https://doi.org/10.1021/cm900166h.
[21] Y. Zhang, Y. Jia, M. Li, L.a. Hou, Influence of the 2-methylimidazole/zinc nitrate hexahydrate molar ratio on the

synthesis of zeolitic imidazolate framework-8 crystals at room temperature, Sci. Rep. 8 (2018) 9597. https://doi.org/10.1038/s41598-018-28015-7.

[22] Y. Li, H. Sun, C. Yang, Z. Yan, J.-Y. Ge, et al., Metal–Organic Frameworks-Based Nanoplatform for Treatment of Breast Cancer, ACS Appl. Nano Mater. 7 (2024) 10532–10542. https://doi.org/10.1021/acsanm.4c00984.

[23] A. Ganesan, J. Leisen, R. Thyagarajan, D.S. Sholl, S. Nair, Hierarchical ZIF-8 materials via acid gas-induced defect sites: synthesis, characterization, and functional properties, ACS Appl. Mater. Interfaces. 15 (2023) 40623–40632. https://doi.org/10.1021/acsami.3c08344.

[24] M.S. Mel'gunov, Application of the simple Bayesian classifier for the N2 (77 K) adsorption/desorption hysteresis loop recognition, Adsorption. 29 (2023) 199–208. https://doi.org/10.1007/s10450-022-00369-5.

[25] K. Noda, M. Ohashi, K. Ishida, Viscosities and densities at 298.15 K for mixtures of methanol, acetone, and water, J. Chem. Eng. Data. 27 (1982) 326–328. https://doi.org/10.1021/je00029a028.

[26] X. Liu, Y. Sun, Effect of ethanol on the morphology and textual properties of ZSM-5 zeolite, Catalysts. 10 (2020) 198. https://doi.org/10.3390/catal10020198.

[27] A.A. Tezerjani, R. Halladj, S. Askari, Different view of solvent effect on the synthesis methods of zeolitic imidazolate framework-8 to tuning the crystal structure and properties, RSC Adv. 11 (2021) 19914–19923. https://doi.org/10.1039/D1RA02856A.

[28] A. Karami, R. Shomal, R. Sabouni, M.H. Al-Sayah, A. Aidan, Parametric study of methyl orange removal using metal–organic frameworks based on factorial experimental design analysis, Energies. 15 (2022) 4642. https://doi.org/10.3390/en15134642.

[29] H. Zhang, X. Shi, J. Li, P. Kumar, B. Liu, Selective dye adsorption by zeolitic imidazolate framework-8 loaded UiO-66-NH2, Nanomaterials. 9 (2019) 1283. https://doi.org/10.3390/nano9091283.

[30] V.A. Tran, A.N. Kadam, S.-W. Lee, Adsorption-assisted photocatalytic degradation of methyl orange dye by zeolite-imidazole-framework-derived nanoparticles, J. Alloys Compd. 835 (2020) 155414. https://doi.org/10.1016/j.jallcom.2020.155414.

[31] M.A. Nazir, M.A. Bashir, T. Najam, M.S. Javed, S. Suleman, et al., Combining structurally ordered intermetallic nodes: Kinetic and isothermal studies for removal of malachite green and methyl orange with mechanistic aspects, Microchem. J. 164 (2021) 105973. https://doi.org/10.1016/j.microc.2021.105973.

[32] E. Santoso, R. Ediati, Z. Istiqomah, D.O. Sulistiono, R.E. Nugraha, et al., Facile synthesis of ZIF-8 nanoparticles using polar acetic acid solvent for enhanced adsorption of methylene blue, Micropor. Mesopor. Mater. 310 (2021) 110620. https://doi.org/10.1016/j.micromeso.2020.110620.

[33] A.S. Al-Wasidi, I.I. AlZahrani, A.M. Naglah, M.G. El-Desouky, M.A. Khalil, et al., Effective removal of methylene blue from aqueous solution using metal-organic framework; modelling analysis, statistical physics treatment and DFT calculations, ChemistrySelect. 6 (2021) 11431–11447. https://doi.org/10.1002/slct.202102330.

[34]A. Alinejad, S. Sadeghi, M. Ghaderpoori, S. Sahebi, A. Ghaderpoury, et al., High adsorption of methylene blue from aqueous solutions using leaf-shaped ZIF-8, J. Environ. Anal. Chem. 101 (2021) 2354–2367. https://doi.org/10.1080/03067319.2019.1702170.

[35] C. Gu, W. Weng, C. Lu, P. Tan, Y. Jiang, et al., Decorating MXene with tiny ZIF-8 nanoparticles: An effective approach to construct composites for water pollutant removal, Chin. J. Chem. Eng. 42 (2022) 42–48. https://doi.org/10.1016/j.cjche.2021.06.004.

[36] M. Ikram, S. Mutahir, M. Humayun, M.A. Khan, J.Y. Al-Humaidi, et al., Facile synthesis of ZIF-67 for the adsorption of methyl green from wastewater: integrating molecular models and experimental evidence to comprehend the removal mechanism, Molecules. 27 (2022) 8385. https://doi.org/10.3390/molecules27238385.